Accurate ^{3}He polarimetry using the Rb Zeeman frequency shift due to the Rb-^{3}He spin-exchange collisions

M. V. Romalis* and G. D. Cates
Department of Physics, Princeton University, Princeton, New Jersey 08544
(Received 6 February 1998)

We describe a method of ^{3}He polarimetry relying on the polarization-dependent frequency shift of the Rb Zeeman resonance. Our method is ideally suited for on-line measurements of the ^{3}He polarization produced by spin-exchange optical pumping. To calibrate the frequency shift we performed an accurate measurement of the imaginary part of the Rb-^{3}He spin-exchange cross section in the temperature range typical for spin-exchange optical pumping of ^{3}He. We also present a detailed study of possible systematic errors in the frequency shift polarimetry. [S1050-2947(98)01010-5]

PACS number(s): 32.80.Bx, 32.30.Dx, 33.25.+k, 33.35.+r

I. INTRODUCTION

Nuclear spin polarized ^{3}He is used in a variety of experiments in atomic, nuclear, and particle physics. Polarized ^{3}He produced by spin exchange with optically pumped Rb metal [1,2] has recently been used for precision measurements of the neutron spin structure functions [3], tests of fundamental symmetries [4], neutron polarizers and analyzers [5], and magnetic resonance imaging (MRI) of the human lungs [6]. Several new experiments designed to measure spin-dependent form factors and structure functions of the neutron and ^{3}He are being developed at Jefferson National Accelerator Facility [7].

In many of these applications, particularly in precision measurements of the neutron and ^{3}He form factors, it is important to know accurately the absolute ^{3}He polarization. At present, the most common method of polarimetry is based on NMR, usually using the technique of adiabatic fast passage (AFP) [8]. While the signal-to-noise ratio provided by this technique is excellent, absolute measurements require a complicated calibration which usually has a limited precision [9]. An alternative method of polarimetry, based on the frequency shift of the Rb Zeeman resonance [also called electron paramagnetic resonance (EPR)] has been developed in [10–12]. Rb-^{3}He spin exchange, responsible for transferring the polarization from Rb to ^{3}He, also shifts the Rb Zeeman frequency. The frequency shift is proportional to the polarization and density of ^{3}He, as well as the imaginary part of the Rb-^{3}He spin-exchange cross section, parametrized by a dimensionless constant κ_0. For ^{3}He densities and polarizations typically used in nuclear physics experiments, the shift is very large (on the order of 20 kHz), and can be measured easily in a typical magnetic field of 20 G, where the Rb EPR frequency is 9 MHz. Thus, once the value of κ_0 is accurately determined, frequency shift polarimetry provides a reliable and accurate method for measuring the ^{3}He polarization without the need for an *in situ* calibration.

Here we extend the technique of frequency shift polarimetry in several ways. We describe a new measurement procedure ideally suited for on-line measurements during optical pumping. It was used at SLAC in the recent neutron spin structure measurement [3,9,13] and has proven to be robust in the accelerator environment. We extend the theoretical treatment of the frequency shift to moderate magnetic fields, where the effect of the hyperfine structure is significant. We report on a new measurement of the Rb-^{3}He spin-exchange constant κ_0. Unlike previous measurements [11,12], our experiment is done in the temperature range typical for spin-exchange optical pumping of ^{3}He. It is also more accurate than previous results. Finally, we discuss in detail possible systematic errors of frequency shift polarimetry, estimate their typical sizes, and describe techniques for minimizing these effects. With these developments the technique of frequency shift polarimetry can now be used easily in experiments requiring very accurate knowledge of the ^{3}He polarization. Frequency shift polarimetry is also useful for making rough measurements of the absolute ^{3}He polarization, since no *in situ* calibration is required. The work presented here provides a practical approach to such measurements as well as an estimate of possible errors.

II. THEORY OF POLARIZATION-DEPENDENT FREQUENCY SHIFT

To calculate the frequency shift due to Rb-^{3}He spin exchange consider the time evolution equation for the density matrix ρ describing the Rb atoms in a magnetic field B directed along the z axis [14,15],

$$\frac{d}{dt}\rho = -2\pi i[A\vec{I}\cdot\vec{S},\rho] - i[\omega_e S_z - \omega_I I_z,\rho] + \Gamma_{SE}(4\alpha\langle\vec{K}\rangle - \vec{C})\cdot\vec{S} + 2i\Gamma_{SE}K_{SE}[\langle\vec{K}\rangle\cdot\vec{S},\rho] + \frac{d'}{dt}\rho. \quad (1)$$

The first two terms give the evolution of the density matrix due to the hyperfine and Zeeman interactions, while the next two terms describe the effect of the Rb-^{3}He spin exchange during binary collisions. The formation of van der Waals molecules is negligible for Rb-^{3}He [2] . Here I and S are the

*Present address: Department of Physics, University of Washington, Seattle, WA 98195.

nuclear and electron spins of the Rb, and K is the ^{3}He nuclear spin. $\Gamma_{SE}=[\mathrm{He}]\langle v\sigma_{SE}\rangle$ is the Rb-He spin-exchange rate per Rb atom, given by the product of the ^{3}He number density [He] and the velocity average of the real part of the spin-exchange cross section σ_{SE}. K_{SE} is the frequency shift parameter defined in [15] as the ratio of the imaginary part of the spin-exchange cross section to its real part. α and $\vec{C}$ are operators acting on the Rb nuclear spin [14]. A is the Rb hyperfine constant, and $\omega_e=g_e\mu_B B/\hbar$ and $\omega_I=g_I\mu_N B/\hbar$ are the electron and nuclear Zeeman frequencies. $d'\rho/dt$ is the contribution to the time evolution from other effects, such as the Rb-Rb spin exchange and optical pumping, which do not depend directly on the ^{3}He polarization. These effects can also cause shifts of the Rb EPR frequency and lead to systematic errors. They are discussed in the Appendix.

Since the ^{3}He nuclear spins are polarized along the z axis, $\langle\vec{K}\rangle=K_z\hat{z}$, the imaginary part of the spin-exchange term can be directly added to the Zeeman term. The real part of the spin-exchange term causes a frequency shift only in second order, i.e., $\Gamma_{SE}(\Gamma_{SE}/\omega_e)$ [14], and is quite negligible. Therefore the frequency shift due to spin exchange is equivalent to a shift by an additional magnetic field

$$B_{SE}=(2K_{SE}\Gamma_{SE}\hbar/g_e\mu_B)K_z, \tag{2}$$

ignoring the contribution from the nuclear Zeeman splitting, which gives a correction on the order of 1×10^{-3}. The value of B_{SE} for typical conditions is about 0.05 G, so in calculating the change of the EPR frequency due to ^{3}He we can use the derivative of the EPR frequency with respect to the magnetic field. Thus, the frequency shift is given by

$$\Delta\nu_{SE}=\frac{d\nu(F,m)}{dB}\,\frac{2\hbar K_{SE}[\mathrm{He}]\langle v\sigma_{SE}\rangle}{g_e\mu_B}K_z, \tag{3}$$

where $\nu(F,m)$ is the EPR frequency of the transition $(F,m\rightarrow F,m-1)$, whose frequency shift is being measured, given by the well-known Breit-Rabi equation [16].

The Rb EPR frequency can also be shifted by the classical magnetic field created by polarized ^{3}He. Only the component of the field parallel to the applied field contributes to the shift to a significant degree. The field is proportional to the ^{3}He magnetization M_{He}, $B_{He}=CM_{He}$, where C is a dimensionless constant which depends on the shape of the cell containing polarized ^{3}He. The shift of the EPR frequency due to this magnetic field is given by

$$\Delta\nu_M=\frac{d\nu(F,m)}{dB}CM_{He}=\frac{d\nu(F,m)}{dB}C[\mathrm{He}]\mu_K K_z/K, \tag{4}$$

where μ_K is the ^{3}He nuclear magnetic moment. The two sources of EPR frequency shift can be combined for a sample of specific shape, since both of them are proportional to the ^{3}He polarization and density. Following the convention in the literature we define a constant κ_0 for a spherical sample by the relation

$$\Delta\nu=\Delta\nu_{SE}+\Delta\nu_M=\frac{8\pi}{3}\,\frac{d\nu(F,m)}{dB}\kappa_0\mu_K[\mathrm{He}]P, \tag{5}$$

where $P=K_z/K$. κ_0 is a dimensionless constant that depends on temperature, but not on the density or the polarization of ^{3}He. The shift parameter K_{He} is absorbed into κ_0. Note that if we ignored all Rb-^{3}He interactions and used only the classical magnetic shift for a sphere ($C=8\pi/3$) then we would get $\kappa_0=1$. So, the value of $\kappa_0\sim6$ can be thought of as an enhancement due to attraction of the Rb electron wave function to the ^{3}He nucleus.

In the limit of low magnetic field $d\nu(F,m)/dB=\mu_B g_e/h(2I+1)$ for all F and m levels, and Eq. (5) reduces to previous definitions in the literature [10–12]. At higher magnetic field the lowest order correction is given by

$$\Delta\nu=\frac{8\pi}{3}\,\frac{\mu_B g_e}{h(2I+1)}\left(1\mp\frac{8I}{(2I+1)^2}\,\frac{\mu_B g_e B}{hA}\right)\kappa_0\mu_K[\mathrm{He}]P \tag{6}$$

for the $F=I+1/2$, $m=\pm F$ state, whose shift is most easily measured in our conditions. For example, for ^{85}Rb $I=5/2$, $A=1012$ MHz, and the correction is 3% for a magnetic field of 20 G.

III. ^{3}He POLARIMETRY

We have developed a new technique for measuring the EPR frequency shift which can be used without significant disruption of the optical pumping process and with a relatively small amount of additional equipment. The setup was implemented at SLAC during the measurement of the neutron spin structure function [3]. It allowed measurements of the polarization without access to the polarized target and proved to be robust under accelerator conditions. Similar setups have been used at Princeton for several experiments.

During spin-exchange optical pumping of ^{3}He [2], the polarization of the Rb vapor is maintained at 60–100 % by optical pumping with a high power laser tuned to the D_1 $(5S_{1/2}\rightarrow5P_{1/2})$ transition in Rb. For definiteness, consider optical pumping with left-circularly polarized light directed parallel to the holding field. Most of the ^{85}Rb atoms are pumped into the $F=3$, $m=3$ state, from which they cannot absorb laser photons. Among the atoms which can absorb the pump photons and are excited to the $5P_{1/2}$ state, most are quenched to the ground state by N_2, which is added to the cell to avoid radiation trapping. A small fraction (3–5 %) decays by emitting a fluorescence photon at either the D_1 or D_2 line. The fluorescence photons are observed through a D_2 filter which blocks the direct light scatter from the laser. By applying a rf field at the frequency of the $m=3\rightarrow2$ transition one can increase the number of atoms in the $m=2$ state which are able to absorb pump photons, and, therefore increase the intensity of the fluorescence. The resonance signal can also be observed at $m=2\rightarrow1$ and other transitions, but it is, in general, much weaker because the population of these states is depleted by optical pumping. Therefore, we always use the $m=3\rightarrow2$ transition (or $m=-2\rightarrow-3$ transition if pumping into the $m=-3$ state).

A typical experimental setup for EPR measurements is shown in Fig. 1. The optical pumping cell, containing a few mg of Rb metal, 9 amg of ^{3}He and 0.08 amg of N_2 [17], is placed in a holding magnetic field B, and is pumped by circularly polarized laser light directed parallel to the holding

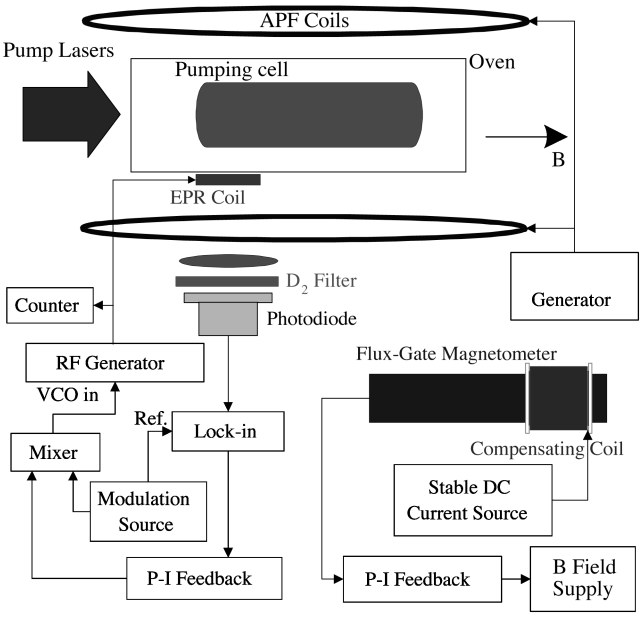

FIG. 1. Typical experimental setup for frequency shift polarimetry.

field. To achieve a desirable Rb number density, $[\mathrm{Rb}] = 10^{14}$–10^{15} cm^{-3}, the cell is placed in an oven and heated to 170–190 °C by flowing hot air. The EPR rf field is created by a coil mounted on the side of the oven. The fluorescence from the cell is detected by a photodiode with a D_2 filter to block the scatter from the pumping lasers. To measure the EPR frequency we use a feedback system [11]. The rf field is generated by a voltage controlled oscillator (VCO), in our case, a Wavetek function generator Model 80. By applying an ac voltage to the input of the VCO we modulate its frequency. A typical value for the amplitude of the frequency modulation is 6 kHz and the modulation frequency is 200 Hz. The photodiode signal is detected by a lock-in amplifier referenced to the modulation frequency. One can show that the lock-in signal is proportional to the derivative of the resonance line shape and crosses zero when the central frequency of the rf field is equal to the EPR frequency. A proportional-integral (PI) feedback circuit adjusts the dc level at the input of the VCO to keep the lock-in signal zero, thus locking the central frequency of the VCO to the EPR resonance. This frequency is measured by a counter and recorded by a computer. To accurately determine the shift of the EPR frequency due to ^{3}He, it is important to keep the applied static magnetic field stable. We used a Bartington flux-gate magnetometer to stabilize the magnetic field. A small coil wound around the head of the magnetometer provided a cancellation field, so the total magnetic field measured by the magnetometer was close to zero. The coil was driven by a precision current source, which served as a reference to which the magnetic field was locked. The output of the magnetometer was connected to a PI feedback circuit controlling the power supply for the Helmholtz coils producing the holding field. The magnetometer was placed sufficiently far from the ^{3}He cell so the magnetic field produced by the polarized ^{3}He at its position was negligible.

To isolate the frequency shift due to the ^{3}He we periodically reversed the direction of the ^{3}He polarization. The reversal was done by the NMR method of adiabatic fast passage [8]. The ^{3}He cell was located inside a pair of AFP coils. The frequency of the rf field created by the coils was swept through the ^{3}He NMR frequency by a HP3325 function generator. The magnitude of the rf field and the frequency sweep rate were adjusted to satisfy the AFP conditions

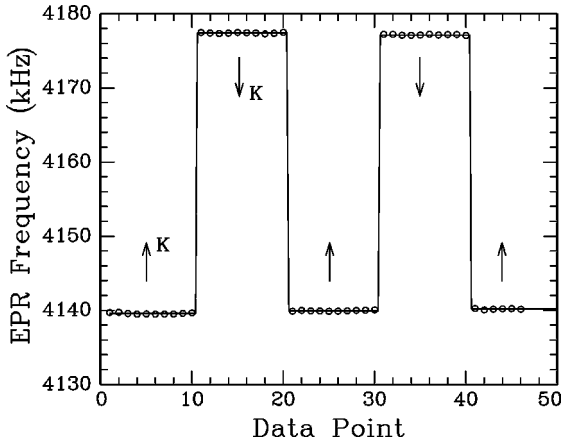

FIG. 2. A typical set of EPR data. The direction of the ^{3}He polarization is periodically reversed by AFP.

$$D\frac{|\vec{\nabla}B_z|^2}{B_1^2} \ll \frac{\gamma\dot{\omega}}{B_1} \ll \gamma B_1, \tag{7}$$

where ω is the rf frequency, B_1 the magnitude of the rf field, $\vec{\nabla}B_z$ is the gradient of the holding field, and D is the ^{3}He diffusion constant. Under these conditions the ^{3}He polarization followed adiabatically the effective field in the rotating frame, and the frequency sweep resulted in a 180° reversal of the polarization. Typical value for B_1 is 100 mG and the frequency sweep rate is 6 kHz/sec. The loss of polarization during AFP reversal was on the order of 0.1%.

The measurement cycle consisted of recording the EPR frequency for about 1 min, then flipping ^{3}He spins by AFP and recording the frequency for another minute. This sequence was repeated several times. A typical data set is shown in Fig. 2. The data are fit allowing a small amount of polarization loss per cycle which is due to the AFP losses and the decay of the polarization during one-half of the cycle when the lasers are pumping in the direction opposite to the ^{3}He polarization. The quality of the data is very high and the size of the frequency shift can be extracted with an error of less than 0.5%.

To determine the ^{3}He polarization from the frequency shift, one has to consider the geometry of the cell containing polarized ^{3}He. Equation (5) is valid only if the cell is spherical. For other geometries, one needs to apply a correction due to the magnetic field shift (4). In general, this correction is not very large, its maximum value (for a long cylinder oriented parallel to B) is about 10%. For a cell of arbitrary shape the magnetic field produced by uniform magnetization filling the cell can be calculated using the technique of scalar magnetic potential [17]. The magnetic field is proportional to the magnetization, $B_{\mathrm{He}} = C(\vec{x})M_{\mathrm{He}}$, with a constant $C(\vec{x})$ which can depend on the position inside the cell. Then κ_0 in Eq. (5) should be replaced by an effective value

$$\kappa_{\rm eff}=\kappa_0+\frac{3}{8\pi}C(\vec{x})-1 \tag{8}$$

and averaged over the region of the cell sampled by the photodiode. If the shape of the cell is given by an ellipsoid of revolution, the correction $C(\vec{x})$ is constant inside the cell. A very long cylinder can be thought of as a limiting case of an ellipsoid and $C(\vec{x})$ is constant in the central region of the cylinder. For other shapes $C(\vec{x})$ is varying within the cell and the uncertainty in the sampling region can lead to errors on the order of 1–2 %, so care should be taken to have a well-defined sampling region. As shown in Fig. 1, the fluorescence is detected in the direction perpendicular to the direction of laser light propagation. By using an appropriate aperture, one can restrict the sampling region in the z direction. This reduces the uncertainty due to variations of the laser intensity along the cell. To properly calculate the depth into the cell sampled by the photodiode, we need to consider the propagation of the unpolarized fluorescence light in the Rb vapor. The Rb spectral linewidth is dominated by pressure broadening due to ^{3}He, and the line profile is given by a Lorentzian

$$\sigma(\nu)=\frac{\sigma_0\Gamma^2}{(\nu-\nu_0)^2+\Gamma^2}, \tag{9}$$

where the half-width Γ is proportional to the ^{3}He pressure [18], and $\sigma_0=cr_ef_2/\Gamma$. Here $f_2\simeq 0.66$ is the oscillator strength of the D_2 transition and r_e is the classical electron radius. In our conditions of strong pressure broadening and optical pumping with broadband light from a diode laser array, the fluorescence light is emitted with the same spectral profile as the absorption profile $\sigma(\nu)$ [19]. As the fluorescence light is propagating toward the surface of the cell its intensity is attenuated according to the equation

$$I(x)=\frac{I_i}{\pi\Gamma\sigma_0}\int d\nu\sigma(\nu)e^{-\sigma(\nu)nx}=I_ie^{-\sigma_0nx/2}I_0(\sigma_0nx/2), \tag{10}$$

where x is the propagation distance, n is the Rb number density, I_i is the initial intensity of the light, and I_0 is the modified Bessel function of zeroth order. In a typical optical pumping cell ([He]$=2.4\times10^{20}$ cm^{-3}, $\Gamma=90$ GHz, $n=4\times10^{14}$ cm^{-3}) $\sigma_0n\approx20$ cm^{-1} and the Rb vapor is optically thick exactly on resonance. The function $I(x)$ drops very fast for small x, but for $x>2$ mm it slows down and drops only as $1/\sqrt{x}$, as shown in Fig. 3. As a result, the cell is sampled relatively uniformly, with only a small part of the signal coming from the region close to the surface of the cell. Equation (10) can be used to calculate the contribution to the EPR signal from different parts of the cell, and the effective average value of κ_0 can be calculated from Eq. (8) [13].

IV. MEASUREMENT OF κ_0

To use the EPR frequency shift for polarimetry we need to know the value of κ_0 for Rb-^{3}He system under typical optical pumping conditions, with the temperature in the range of 170–190 °C. Previous measurements were performed over a temperature range of 40–80 °C [11,12], and it was found that κ_0 has a mild temperature dependence. Therefore we performed a new measurement in the temperature range of 110–175 °C.

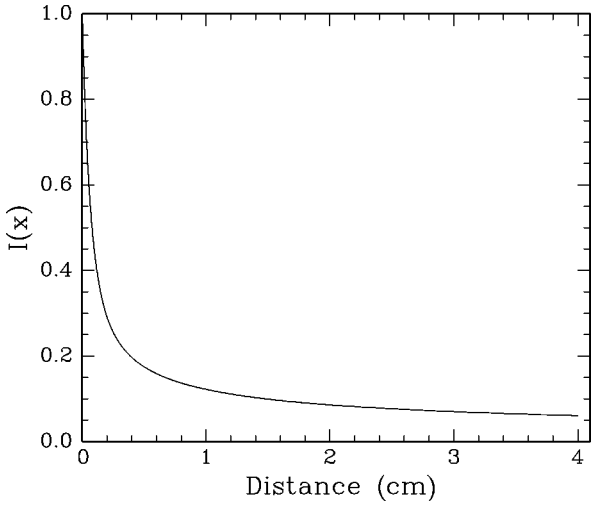

FIG. 3. The attenuation of the intensity of the fluorescence light emitted by the Rb atoms in the optical pumping cell as it propagates through the cell.

The measurement used an interplay between the spin exchange and magnetic field sources of the frequency shift, a technique first implemented in [12]. For a spherical sample the frequency shift is given by Eq. (5). For a sample of another shape we can imagine a sphere around the EPR detection region which gives the same shift plus a shift due to the remaining parts of the sample. Since the ^{3}He atoms in these parts do not come into direct physical contact with the Rb atoms in the detection region, they cannot contribute to the shift through the spin exchange. They only contribute through the classical magnetic field shift, which can be calculated based on the geometry of the sample. Making two measurements with different geometry we can separate the magnetic field shift from the shift due to the spin exchange,

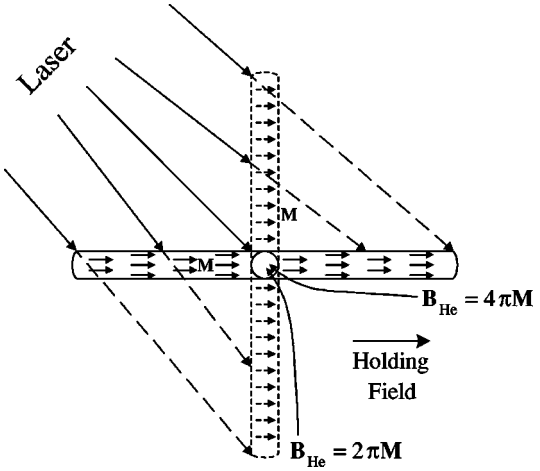

FIG. 4. Schematic of the experimental setup used for measurement of κ_0. The cell was periodically rotated between the two orientations shown in solid and broken lines. The value of the magnetic field created by polarized ^{3}He is indicated for each orientation.

and determine the value of κ_0. We used a long cylinder to make the measurements as shown in Fig. 4. The magnetic field produced by a uniform magnetization M parallel to the axis of a very long cylinder is $B=4\pi M$. For a cylinder magnetized perpendicular to its axis the field is $B=2\pi M$. The field inside a uniformly magnetized sphere is $B=8\pi M/3$. The frequency shifts for the longitudinal and transverse orientations are given by

$$\Delta\nu_L=\frac{d\nu(F,m)}{dB}\mu_K[\mathrm{He}]P\left[\frac{8\pi}{3}\kappa_0+\left(4\pi-\frac{8\pi}{3}\right)\right], \quad (11)$$

$$\Delta\nu_T=\frac{d\nu(F,m)}{dB}\mu_K[\mathrm{He}]P\left[\frac{8\pi}{3}\kappa_0+\left(2\pi-\frac{8\pi}{3}\right)\right]. \quad (12)$$

Introducing polarization to frequency shift conversion constants $\Delta\nu_L=PK_L$, $\Delta\nu_T=PK_T$, we can cancel the polarization of ^{3}He and obtain $\kappa_0=3(K_L+K_T)/8(K_L-K_T)-1/8$.

A cylindrical cell 1.2 cm in diameter and 18 cm long was prepared for the experiment. The cell contained a few mg of Rb metal in natural abundance, 8.4 amg of ^{3}He, and 0.08 amg of N_2. The magnetic field produced by a uniform magnetization in the cell differed from the field for an infinite cylinder by less than 0.6%. Variations of the magnetic field inside the sampling region were less than 0.03%. To change the orientation of the magnetization, the cell was rotated with respect to the holding field as shown in Fig. 4. The EPR detector placed near the center of the cell consisted of a 2 cm diameter rf coil, a light collecting lens, a D_2 filter, and a photodiode. The electronics was similar to the polarimetry setup described above, except for the field locking mechanism. Since the value of κ_0 depends on the difference between the EPR shifts in the two orientations, which is only 16% of the total shift, the frequency shifts had to be measured with much higher accuracy. To achieve sufficient accuracy it was necessary to keep the field stable to one part in 10^6, which exceeded the stability of the current source. Therefore the field was locked to a Cs magnetometer which used a rf generator as a reference source. The principle of operation of the Cs magnetometer is also based on the EPR resonance [11,20]. The field locking is essentially an inversion of the above mentioned feedback scheme, where the rf frequency is kept constant and the magnetic field is locked to the resonance. The rf generator for the Cs magnetometer was synchronized with the counter used to measure the Rb EPR frequency to avoid relative drifts. The magnetometer was placed sufficiently far from the He cell to avoid spurious feedback due to the magnetic field created by the ^{3}He. The magnitude of the frequency shift was measured by periodically flipping ^{3}He polarization with AFP. During the measurement the cell was also frequently rotated by 90° from the longitudinal to the transverse orientation. To keep the laser illumination constant, it was positioned at 45° to the magnetic field in the plane of the cell rotation.

The measurement procedure consisted of a combination of the following three actions: measuring the EPR frequency (M), flipping the spins by AFP (F), and rotating the cell (R). It was important to properly take into account the changes of the polarization during the measurement due to the optical pumping and AFP losses, since they were significant compared to the required accuracy. Several measurement sequences were tried and it was found that the best cycle was $MFMFMR$, which was repeated many times during the measurement. The data from a typical run are shown in Fig. 5. Let us follow the polarization during a measurement cycle. For definiteness, we start in the longitudinal orientation with the ^{3}He spins pointing in the direction of optical pumping, parallel to the magnetic field B, and having a polarization P. During the measurement of the EPR frequency the polarization changes due to optical pumping and spin relaxation. We will parametrize the change by a fractional polarization loss per second, so after a time T the polarization will be $P(1-S_{UL}T)$. The first subscript refers to the orientation of the spins (up or down) with respect to the magnetic field and the second subscript refers to the orientation of the cell (longitudinal or transverse). We also introduce corresponding constants S_{DL} for ^{3}He spins opposite to the magnetic field in the longitudinal orientation of the cell, and S_{DT} and S_{UT} for the transverse orientation of the cell. Since the change of the polarization during the whole measurement sequence is relatively small (about 5%), we will assume that the fractional loss parameters remain constant. For AFP losses we introduce a fractional loss constant α per flip. Then the frequency shift at various points in the cycle is given by (see Fig. 5 for notation)

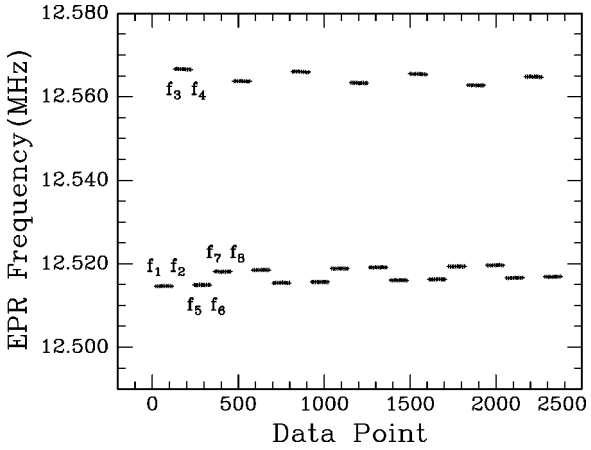

FIG. 5. A typical set of data used to extract the value of κ_0. Frequencies refer to Eq. (13).

$$\begin{aligned}
f_1&=f_L-PK_L,\\
f_2&=f_L-P(1-S_{UL}T)K_L,\\
f_3&=f_L+P(1-S_{UL}T)(1-\alpha)K_L,\\
f_4&=f_L+P(1-S_{UL}T)(1-\alpha)(1-S_{DL}T)K_L,\\
f_5&=f_L-P(1-S_{UL}T)(1-\alpha)^2(1-S_{DL}T)K_L, \quad (13)\\
f_6&=f_L-P(1-S_{UL}T)(1-\alpha)^2(1-S_{DL}T)(1-S_{UL}T)K_L,\\
f_7&=f_T-P(1-S_{UL}T)(1-\alpha)^2(1-S_{DL}T)(1-S_{UL}T)K_T,\\
f_8&=f_T-P(1-S_{UL}T)(1-\alpha)^2(1-S_{DL}T)\\
&\quad\times(1-S_{UL}T)(1-S_{DT}T)K_T,
\end{aligned}$$

where f_L and f_T are the baseline EPR frequencies in the longitudinal and transverse orientations. During the first cycle we directly measure three quantities: $M_1=(f_1+f_2)/2$, $M_2=(f_3+f_4)/2$, and $M_3=(f_5+f_6)/2$. We can extract $f_L=(M_1+2M_2+M_3)/4$ if we expand everything to first order, since all losses are much less than a percent. We also calculate the frequency shift before and after the longitudinal cycle: $\Delta f_{BL}=f_L-M_1=PK_L(1-S_{UL}T/2)$, and $\Delta f_{AL}=f_L-M_3=PK_L(1-S_{UL}T)(1-\alpha)^2(1-S_{DL}T)(1-S_{UL}T/2)$. We repeat the same procedure for the next cycle, done in the transverse orientation. Now we calculate

$$A_1=\frac{\Delta f_{AL}-\Delta f_{BT}}{\Delta f_{AL}+\Delta f_{BT}}=\frac{K_L-K_T(1-S_{UL}T/2)(1-S_{DT}T/2)}{K_L+K_T(1-S_{UL}T/2)(1-S_{DT}T/2)}, \tag{14}$$

where again we used first order expansion. Repeating the cycle one more time we can also form the ratio $A_2=(\Delta f_{BL}-\Delta f_{AT})/(\Delta f_{AT}+\Delta f_{BL})$. Averaging the two asymmetries we get

$$\overline{A}=\frac{A_1+A_2}{2}=\frac{K_L-K_T}{K_L+K_T}\left\{1-\frac{K_LK_T}{(K_L+K_T)^2}\left(\frac{S_{UL}+S_{DT}}{2}T\right)^2\right\}, \tag{15}$$

to the lowest nontrivial order. So, with this combination of measurements, the correction is second order in the amount of loss per cycle. Since the total loss during a complete cycle $(2S_{UL}T+S_{DL}T+2\alpha)$ is about 0.5%, this correction is negligible. We usually repeated the cycle 10–30 times to reduce the random measurement noise to about 0.4%. For an infinite cylinder the value of κ_0 is given by $\kappa_0=3/(8\overline{A})-1/8$. For our cell the field was slightly different ($B_{\rm He}=12.542M$ for the longitudinal and $6.295M$ for the transverse orientation), so $\kappa_0=0.3728/\overline{A}-0.1243$.

Various systematic checks were performed during the experiment. The biggest systematic uncertainty comes from the temperature of the cell. A 50 W diode laser was used for optical pumping and EPR detection, and it caused a substantial heating of the cell. The temperature of the cell was measured by 4 resistive temperature detectors (RTDs) mounted along its length. The RTD used to control the temperature of the oven was located near the center of the cell. It was attached to the cell with a high thermal conductivity compound and shielded from the air flow and direct laser light by a Teflon screen. The temperatures of the other RTDs differed by less than 5 °C. It is particularly important to study the asymmetry in temperature between the transverse and longitudinal orientations of the cell. Given the temperature dependence of κ_0, an asymmetry of 1°C will cause a 1.3% error in determination of κ_0. Therefore the temperature was carefully recorded during the measurement cycle. It was found that the asymmetry was less than 0.6 °C. Another way to check for significant temperature asymmetry is to vary the measurement period T, reducing it to the point where the temperature asymmetry does not have enough time to develop. We changed T from 3 to 100 sec and have not seen changes in κ_0 of more than 0.5%. We also studied the dependence of κ_0 on the power of the diode laser while keeping the temperature measured by the RTD constant. Reducing the power of the laser by about a factor of 2 reduced the value of κ_0 by 0.7%. This change can be explained by a 5 °C reduction of the temperature inside the cell, which is in agreement with an estimate based on the heat conductivity of the glass walls of the cell.

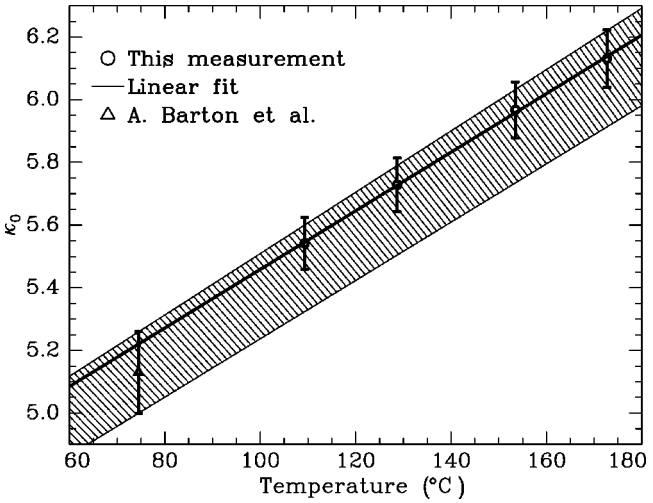

FIG. 6. The results of our measurement of κ_0 compared with previous experiments. The hatched region is obtained using the result of [12] and by assuming that the temperature dependence measured in [11] is valid up to 180 °C.

The alignment of the cell with respect to the magnetic field was checked by mapping the frequency shift vs angle near the transverse and longitudinal orientations. It was found that the alignment was better than 1° causing an error of less than 0.1%. The Earth's magnetic field rotated the magnetization vector from the horizontal plane by 1° for the data taken with a holding field of 27 G and by 2.5° for the data at 11 G causing an error of less than 0.3% in the worst case. To check for the possibility of a polarization gradient across the cell, several EPR measurements were done along its axis. It was found that the changes in the EPR frequency shift along the length of the cell were on the order of 0.2% and were monotonic from one end of the cell to the other. So they could not cause a significant error in the value of κ_0. They were probably due to a temperature gradient since the air inlet was located near one end of the cell. We also checked the dependence of κ_0 on the magnitude of the holding magnetic field, the direction of the circular polarization of the laser light, the magnitude of the ^{3}He polarization (from 25% to 45%), and the method of mounting the RTDs. The biggest difference was observed in the case of the ^{3}He polarization, and was equal to 0.7%. In all other cases we have not seen any changes at the level of our statistical precision of 0.4%.

We studied the temperature dependence of κ_0 by making measurements at four different temperatures, from 110 °C to 172 °C. Our results are shown in Fig. 6. They can be parametrized by the linear fit

$$\kappa_0=4.52+0.009\,34[T(^\circ\mathrm{C})]. \tag{16}$$

The error in κ_0 is dominated by systematic errors. Our estimates of the systematic effects indicate that the largest errors are due to the temperature asymmetry (0.8%) and the absolute temperature uncertainty (0.7%). We also add in quadra-

TABLE I. Summary of the systematic errors in the measurement of κ_0.

Error source	Error in κ_0 at 175 °C
Calculated systematic errors	
Temperature asymmetry	0.8%
Absolute temperature	0.7%
Alignment	0.2%
Observed systematic variations	
Laser power	0.7%
Measurement period	0.5%
Polarization	0.7%
Total	1.5%

ture all observed systematic variations of κ_0 which exceeded our statistical resolution of 0.4%. Although these variations are likely due to the systematic effects considered above or to random fluctuations, we cannot exclude the possibility that the origin of some of these variations has not been identified. The total error of our measurement is 1.5%, the components of which are summarized in Table I.

Figure 6 also shows previous measurements of κ_0 for Rb-^{3}He. Barton *et al.* [12] measured κ_0 at 74.5 °C with an accuracy of 2.5% using an experimental technique similar to ours. The temperature dependence of κ_0 has been measured by Newbury *et al.* [11] in the range of 40–80 °C, but their value of κ_0 had a much larger absolute error.

The hatched region in Fig. 6 is obtained by using the value of κ_0 from [12] and extrapolating the temperature dependence measured in [11] to 180 °C. As can be seen, our results for the absolute value and the temperature dependence of κ_0 are in very good agreement with previous measurements.

V. CONCLUSION

We have presented a method of ^{3}He polarimetry based on the frequency shift of the Rb Zeeman resonance. The method is well suited for precision polarimetry of ^{3}He polarized by spin exchange with optically pumped Rb. We discuss in detail the implementation of the technique and possible systematic errors. The constant κ_0, necessary for the calibration of our method, is measured with an accuracy of 1.5%. With these developments, frequency shift polarimetry becomes an attractive alternative to more traditional NMR methods of polarimetry.

ACKNOWLEDGMENTS

We would like to acknowledge discussions with Will Happer, Todd Smith, and Tim Chupp. This research was supported by the U.S. DOE under Contract No. DE-FG02-90ER40557 and the NSF under Contract No. NSF-9413901.

APPENDIX: EFFECTS OF ADDITIONAL FREQUENCY SHIFTS

In this appendix we discuss several effects which can cause systematic errors in the frequency shift polarimetry. In addition to the shift caused by polarized ^{3}He, the Rb EPR frequency is shifted by other effects, the largest of which are the Rb-Rb spin exchange and the light shift due to optical pumping. As will be seen from the estimates below, these shifts are comparable to the shift produced by polarized ^{3}He and can potentially cause substantial errors. To significantly reduce their effect, we periodically reverse the direction of the ^{3}He polarization by AFP, while keeping other optical pumping parameters constant. The frequency shift due to ^{3}He is determined from the difference between the Rb EPR frequencies for the two directions of the ^{3}He polarization. Because Rb-^{3}He spin exchange is a very slow process, to a first approximation the direction and value of the ^{3}He polarization does not affect any other processes in the optical pumping cell, and the size of these additional shifts does not change when the ^{3}He polarization is flipped. Here we consider under what conditions this approximation is valid.

One can show [2] that the equilibrium polarization of the Rb vapor is given by

$$P_{\mathrm{Rb}}=\frac{R+\Gamma_{\mathrm{SE}}P_{\mathrm{He}}}{R+\Gamma_{\mathrm{SD}}+\Gamma_{\mathrm{SE}}}, \tag{A1}$$

where Γ_{SD} is the Rb spin destruction rate and R is the optical pumping rate. For typical optical pumping conditions ($[\mathrm{He}]=2.4\times10^{20}$ cm^{-3}, $[\mathrm{Rb}]=4.3\times10^{14}$ cm^{-3}, $T=453$ K) the rates are: $\Gamma_{\mathrm{SD}}=725$ s^{-1}, $\Gamma_{\mathrm{SE}}=16$ s^{-1}, using the rate constants from [21]. The optical pumping rate in the front of the cell is usually 10–100 times larger than Γ_{SD}, so $\Gamma_{\mathrm{SE}}\sim10^{-3}R$. However, as the laser power is absorbed in the cell, the pumping rate drops, and the value of the Rb polarization becomes more sensitive to the ^{3}He polarization.

The largest contribution to $d'\rho/dt$ in Eq. (1) comes from the Rb-Rb spin exchange [14]

$$\frac{d}{dt}\rho=\Gamma_{\mathrm{Rb}}(4\alpha\langle\vec{S}\rangle-\vec{C})\cdot\vec{S}+2i\Gamma_{\mathrm{Rb}}K_{\mathrm{Rb}}[\langle\vec{S}\rangle\cdot\vec{S},\rho], \tag{A2}$$

where $\Gamma_{\mathrm{Rb}}=[\mathrm{Rb}]\overline{v\sigma}_{\mathrm{Rb\text{-}Rb}}$ is the spin-exchange rate and K_{Rb} is the frequency shift parameter. The real part of this expression affects the frequency shift only in the second order, i.e., $\delta\nu\sim\nu_{\mathrm{EPR}}(\Gamma_{\mathrm{Rb}}/\omega_e)^2$ [14]. Using $\sigma_{\mathrm{Rb\text{-}Rb}}=2\times10^{-14}$ cm^2 [22] we get at 180 °C a frequency shift of only $\delta\nu=13$ Hz. The imaginary part of Eq. (A2) contributes directly to the frequency shift. The shift parameter K_{Rb} for the Rb-Rb spin exchange is calculated by Kartoshkin [23]: $K_{\mathrm{Rb}}=-0.14$. Using this number, and assuming that $\langle\vec{S}\rangle=1/2$, we estimate that the shift due to the imaginary part of Eq. (A2) is $\delta\nu'=\Gamma_{\mathrm{Rb}}K_{\mathrm{Rb}}/2\pi(2I+1)=1.5$ kHz, which is comparable to a typical shift of 20 kHz due to ^{3}He. However, if the changes in the Rb polarization correlated with the direction of the ^{3}He polarization are on the order of 10^{-2}, this is not a significant source of systematic error, provided that one determines the frequency shift by flipping the direction of the ^{3}He polarization. Therefore we need to have $R\geqslant10^2\Gamma_{\mathrm{SE}}$.

Another source of the Rb EPR frequency shift is due to the light shift produced by the optical pumping laser. The evolution of the Rb density matrix due to optical pumping is given by [24,25]

$$\frac{d}{dt}\rho = R[\alpha(1+2\vec{s}\cdot\vec{S})-\rho]+i\Omega[(\tfrac{1}{2}-\vec{s}\cdot\vec{S}),\rho], \quad \text{(A3)}$$

where R and Ω are the real and imaginary parts of the complex pumping rate $\tilde{R}$,

$$\tilde{R} = R + i\Omega = r_e c f_1 \int \frac{\Phi(\nu)d\nu}{\Gamma + i(\nu-\nu_0)}. \quad \text{(A4)}$$

Here $\Phi(\nu)$ is the spectral flux of the pumping photons, s is the mean photon spin of the pumping light, and $f_1 \simeq 0.33$ is the oscillator strength of the D_1 transition. Again, only the complex part of this expression contributes significantly to the frequency shift. The light shift has a dispersion shape and vanishes if the center of the laser spectral profile coincides with the optical line center. To estimate the maximum possible value of the light shift we consider optical pumping with a diode laser array and assume that its spectral profile can be approximated by a Gaussian with a full width at half maximum (FWHM) of 2 nm. For laser power density of 5 W/cm^2 and $\Gamma = 90$ GHz we estimate that the maximum frequency shift due to optical pumping is $\delta\nu_{LS} = \Omega/2\pi(2I+1) = 2.4$ kHz and occurs for laser detuning of 0.6 nm. This number is again comparable to the frequency shift produced by ^{3}He. The intensity of the light can be affected by the reversal of the ^{3}He polarization because the absorption of the light in the cell depends on the Rb polarization

$$\frac{\partial\Phi(\nu,z)}{\partial z} = -[\mathrm{Rb}]\sigma(\nu)\Phi(\nu,z)[1-sP_{\mathrm{Rb}}(z)], \quad \text{(A5)}$$

which, in turn, depends on the ^{3}He polarization through Eq. (A1). Thus we need to ensure that the intensity of the optical pumping light does not vary appreciably when the direction of the ^{3}He polarization is reversed.

The sources of the systematic error considered above are small if the pumping rate R is much larger than the spin-exchange rate Γ_{SE}. To ensure that this condition is satisfied, the fluorescence should be detected in the front of the optical pumping cell, where the intensity of the laser light is maximal.

[1] M. A. Bouchiat, T. R. Carver, and C. M. Varnum, Phys. Rev. Lett. **5**, 373 (1960).
[2] T. Walker and W. Happer, Rev. Mod. Phys. **69**, 629 (1997).
[3] K. Abe *et al.* (the E-154 Collaboration), Phys. Rev. Lett. **79**, 26 (1997); Phys. Lett. B **404**, 377 (1997).
[4] T. E. Chupp, R. J. Hoare, R. L. Walsworth, and Bo Wu, Phys. Rev. Lett. **72**, 2363 (1994).
[5] G. L. Greene, A. K. Thompson, and M. S. Dewey, Nucl. Instrum. Methods Phys. Res. A **356**, 177 (1995).
[6] H. Middleton, Magn. Reson. Med. **33**, 271 (1995).
[7] B. Fillipone *et al.* (unpublished).
[8] A. Abragam, *Principles of Nuclear Magnetism* (Oxford University Press, New York, 1961).
[9] M. V. Romalis *et al.*, Nucl. Instrum. Methods Phys. Res. A **402**, 260 (1998).
[10] S. R. Schaefer, G. D. Cates, T. R. Chien, D. Gonatas, W. Happer, and T. G. Walker, Phys. Rev. A **39**, 5613 (1989).
[11] N. R. Newbury, A. S. Barton, P. Bogorad, G. D. Cates, M. Gatzke, H. Mabuchi, and B. Saam, Phys. Rev. A **48**, 558 (1993).
[12] A. S. Barton, N. R. Newbury, G. D. Cates, B. Driehuys, H. Middleton, and B. Saam, Phys. Rev. A **49**, 2766 (1994).
[13] M. V. Romalis, Ph.D. thesis, Princeton University, 1997 (unpublished).
[14] W. Happer and A. C. Tam, Phys. Rev. A **16**, 1877 (1977).
[15] L. C. Balling, R. J. Hanson, and F. M. Pipkin, Phys. Rev. **133**, A607 (1964).
[16] G. K. Woodgate, *Elementary Atomic Structure* (Oxford University Press, Oxford, 1989).
[17] J. D. Jackson, *Classical Electrodynamics* (John Wiley, New York, 1975), p. 193.
[18] M. V. Romalis, E. Miron, and G. D. Cates, Phys. Rev. A **56**, 4569 (1997).
[19] N. Allard and J. Kielkopf, Rev. Mod. Phys. **54**, 1103 (1982).
[20] W. Farr and E. W. Otten, Appl. Phys. **3**, 367 (1974).
[21] A. B. Baranga, S. Appelt, M. V. Romalis, C. J. Erickson, A. R. Young, G. D. Cates, and W. Happer, Phys. Rev. Lett. **80**, 2801 (1998).
[22] J. Vanier and C. Audoin, *Quantum Physics of Atomic Frequency Standards* (Hilger, Bristol, 1989).
[23] V A. Kartoshkin, Opt. Spektrosk. **79**, 26 (1995) [Opt. Spectrosc. **79**, 22 (1995)].
[24] W. Happer and B. S. Mathur, Phys. Rev. **163**, 12 (1967).
[25] S. Appelt, A. B. Baranga, C. J. Erickson, M. V. Romalis, A. R. Young, and W. Happer, Phys. Rev. A **56**, 1412 (1998).